

Chapter 5

Influence of Cholesterol on DOPC Membranes

5.1 Introduction

As discussed in chapter 1, ternary mixtures of cholesterol with a lipid with saturated hydrocarbon chains, such as DPPC, and a lipid with unsaturated chains, such as DOPC, have been widely studied in order to understand the formation of cholesterol-rich domains in biomembranes [1, 2, 3, 4]. We have also studied this ternary system and have observed for the first time the coexistence of two fluid phases using diffraction technique. This will be discussed in detail in chapter 6. Two-phase coexistence in this system has been seen in microscopy studies on giant unilamellar vesicles (GUVs). One of these phases is believed to be rich in the unsaturated lipid and the other in the saturated one. In order to understand the structure and composition of the coexisting phases in the ternary mixtures it is necessary to establish the phase behaviour of the two binary mixtures. We have already discussed the phase behaviour of DPPC-cholesterol mixtures in chapter 3. In this chapter, we discuss the phase behaviour of binary mixtures of cholesterol with DOPC. We summarize earlier studies on this system in section 5.2. The experimental results obtained from DOPC-cholesterol mixtures are described in section 5.3. Finally we discuss the electron density profiles obtained from x-ray diffraction data in section 5.4.

5.2 Earlier studies

The presence of unsaturated lipids, such as DOPC and POPC, in raft forming compositions has led to a large number of studies of the influence of cholesterol on their model membranes using a variety of experimental techniques [5, 6, 7, 8, 9, 10, 11, 12, 13]. DOPC and DOPC-cholesterol mixtures form a lamellar phase at around ambient temperature. Although the presence of cholesterol does not alter the phase behaviour over a wide range of cholesterol concentrations ($X_c < 50$ mol%), the bilayer properties do change with increasing X_c . For example, the d-spacing of the lamellar phase was found to increase from 61 Å to 68 Å as X_c was increased from 0 to 50 mol% [14]. However, no significant change in the bilayer thickness has been found in a small angle neutron scattering (SANS) study [7]. Angle resolved fluorescence depolarization techniques have shown that the orientational order parameter of the probe molecules increases and that the orientational distribution function of these molecules gets narrowed in the presence of cholesterol [8, 9]. In a nuclear magnetic resonance (NMR) study, lateral diffusion of DOPC molecules was found to decrease with increasing X_c [10, 15]. Similar behaviour was also seen in a fluorescence correlation spectroscopy (FCS) study on GUVs [16]. For example, from FCS on DOPC-cholesterol GUVs, the average diffusion coefficient of fluorescence probe molecule was found to decrease from 6.5×10^{-12} to 2.5×10^{-12} m²/s as X_c was increased from 0 to 60 mol%.

Phase transition from a lamellar to a hexagonal structure has been found in DOPC-cholesterol mixtures at high cholesterol concentrations (> 50 mol%) and at high temperatures ($\sim 80^\circ\text{C}$). This transition was detected using differential scanning calorimetry (DSC) and x-ray diffraction techniques [14]. We will not discuss the non-lamellar phases of DOPC-cholesterol mixtures and shall confine our attention to the lamellar phase of their mixtures, which is more relevant to the formation of cholesterol-rich domains in ternary mixtures that will be discussed in chapter 6.

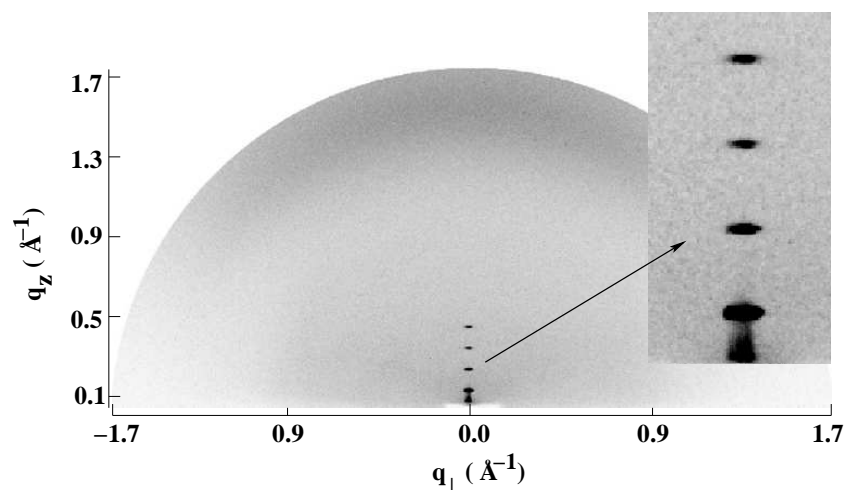


Figure 5.1: Diffraction pattern of the fluid (L_α) phase rich in cholesterol obtained from DOPC–cholesterol mixture ($X_c = 30$ mol%, $T = 10^\circ\text{C}$, $\text{RH} = 98\%$). The inset shows the small angle region of the diffraction pattern on an expanded scale.

5.3 Experimental results

A systematic investigation on mixtures of cholesterol with DOPC was carried out using x-ray diffraction technique. Mixtures with X_c of 0, 5, 10, 15, 20, 25 and 30 mol% were studied. Diffraction experiments were done with aligned samples as described in chapter 2, at temperatures varying from 40 to 5°C at 98% relative humidity (RH). The 1,2-Di[*cis*-9-octadecenoyl]-sn-glycerol-3-phosphatidylcholine (DOPC) which we used for the experiments has a *cis*-double bond at the 9th position in both the hydrocarbon chains. The main transition temperature of this DOPC was reported to be -18.3°C [17]. Therefore, we have obtained the fluid (L_α) phase throughout the temperature range studied. Diffraction pattern from the fluid phase of DOPC and DOPC–cholesterol mixtures consists of four reflections in the small angle region. Wide angle reflections were not seen in our aligned experimental geometry even after a long exposure, as in the fluid phase of all samples studied (Fig. 5.1). Although the number of reflections in the small angle region do not increase with increasing cholesterol content, the relative intensities of these reflections do change with X_c . The d-spacings obtained from DOPC–cholesterol mixtures at various temperatures are summarized in table 5.1. Relative intensities of the reflections obtained from the diffraction data are given in tables 5.2 and 5.3.

Table 5.1: The spacings d (Å) obtained from the diffraction data of DOPC–cholesterol mixtures at various temperatures. Relative humidity was kept fixed at 98 ± 2 %. The error in d is ± 0.3 Å.

T°C	X_c (mol%)						
	0	5	10	15	20	25	30
40	53.2	52.9	53.9	54.3	55.3	53.0	54.9
35	54.1	53.3	54.3	54.3	54.9	53.3	55.8
30	53.8	53.3	54.3	54.2	54.5	53.6	55.4
25	54.0	53.8	53.8	54.0	54.3	54.0	55.4
20	54.3	54.9	54.9	55.4	55.3	55.3	56.4
15	54.3	54.7	55.6	55.3	56.0	55.3	56.6
10	54.2	54.4	55.6	55.3	56.0	55.3	56.6
5	54.2	53.8	55.0	55.3	55.8	55.3	56.6

Table 5.2: The observed magnitude of structure factors $F(h)$ ($= \sqrt{\frac{I(h)}{I(h=1)}} \times 100$) calculated from the diffraction data at various X_c ($T = 10^\circ\text{C}$, $\text{RH} = 98\%$). As discussed in the text, the phases of these reflections do not change with X_c .

X_c	F(1)	F(2)	F(3)	F(4)
0	10	4.5	5.3	3.2
5	10	4.7	4.6	3.2
10	10	4.5	4.9	4.0
15	10	4.7	4.8	4.1
20	10	4.1	3.5	3.2
25	10	4.0	3.5	3.3
30	10	4.2	2.9	3.7
phases	-	-	+	-

Table 5.3: The observed magnitude of structure factors $F(h)$ ($= \sqrt{\frac{I(h)}{I(h=1)}} \times 100$) calculated from the diffraction data at various temperatures ($X_c = 30$ mol%, $RH = 98\%$). As discussed in the text, the phases of these reflections do not change with temperature.

T°C	F(1)	F(2)	F(3)	F(4)
40	10	4.0	2.8	3.2
30	10	4.3	2.9	3.5
25	10	3.9	2.9	3.8
20	10	4.3	3.0	3.7
15	10	4.3	3.1	3.8
10	10	4.2	2.9	3.7
phases	-	-	+	-

5.4 Discussion

The results presented here clearly show that DOPC and DOPC–cholesterol mixtures exhibit a fluid phase throughout the temperature range studied. Electron density profiles were calculated from the diffraction data presented in tables 5.2 and 5.3. Phases of the reflections were obtained by fitting the experimental intensities with the three delta function model, as discussed in chapter 2. Diffraction patterns of all samples show only four lamellar reflections in the small angle region. Therefore, it was not possible to obtain a good fit from the model. Since there are four reflections, only 2^4 ($= 16$) combinations of phases are possible and we have calculated the electron density profile for all the combinations of the phases by fixing the phase of the 1st order reflection (strongest peak) (Fig. 5.2). Profile (a) in Fig. 5.2 shows similar electron density in both the head group and water regions which is unrealistic, as the electron density of the head group region is expected to be much higher than that of water. The bilayer thickness is unreasonable in profiles (b) and (d) of Fig. 5.2, as d-spacing in this system is found to be ~ 54 Å. Therefore, we can rule out these two profiles. All profiles in the right panel can be discarded, as we would expect the lowest electron density at the center of the bilayer containing the terminal methyl group. Therefore, only one combination of phases (- - + -) gives a realistic electron density profile, as shown in Fig. 5.2 c, which is also in agreement with those presented in ref. [18]. This combination of phases remains

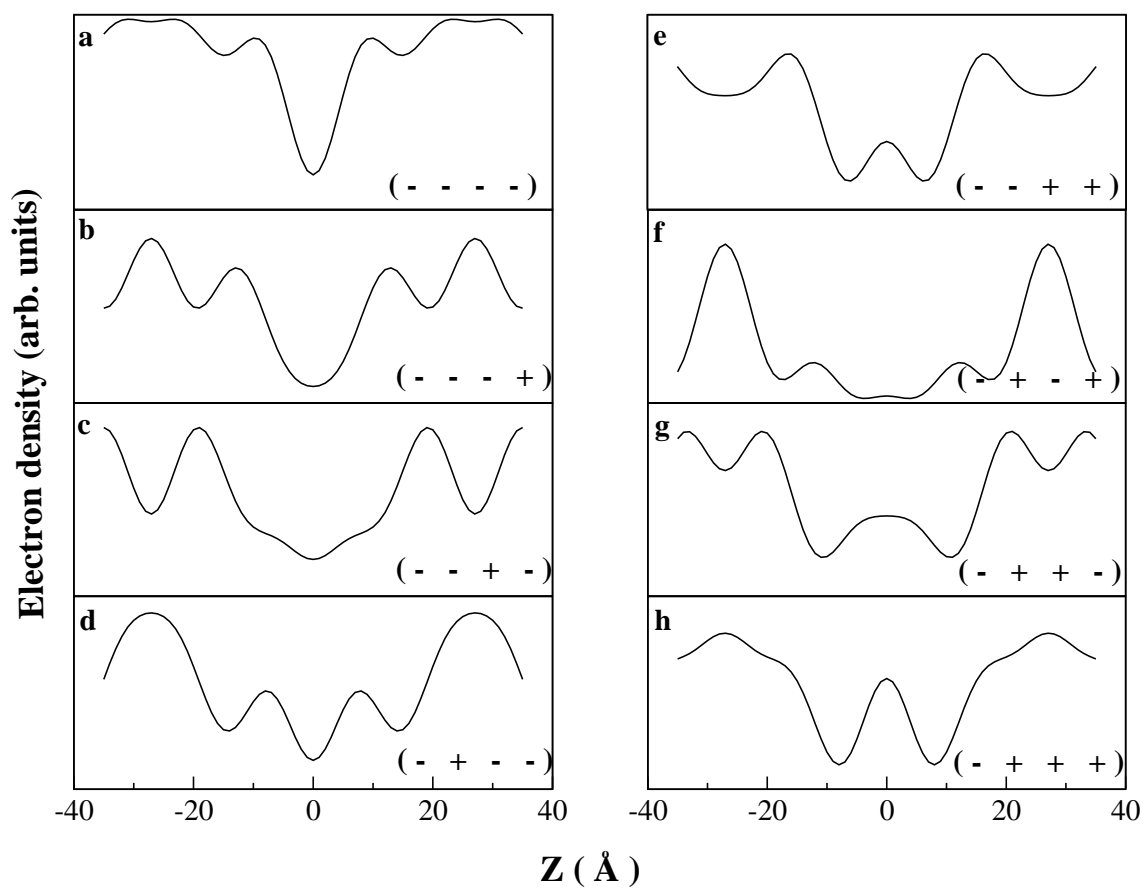


Figure 5.2: Calculated electron density profiles using all combinations of phases. Only the profile shown in *c* is reasonable and gives a correct bilayer thickness. Same set of phases as given in *c* was also obtained from the model.

unchanged for all samples studied. The electron density of the terminal methyl group of DOPC bilayer in the fluid phase shows a broader shallow trough, compared to that of distearoyl phosphatidylcholine (DSPC) of same chain length [19]. The presence of a kink in the hydrocarbon chains of DOPC might lower the effective electron density of the chain region, resulting in the broad shallow trough in the electron density profile as mentioned above. Electron density profiles of DOPC bilayers presented in Fig. 5.3 as a function of cholesterol content show no significant change with X_c . From these profiles, bilayer thickness is found to be 40 Å at all X_c and it is comparable with the thickness in pure DOPC bilayer, in good agreement with earlier studies [7, 4]. As can be seen in Fig. 5.3, the dip in the electron density profile corresponding to the terminal methyl group is very broad in pure DOPC and becomes narrower as X_c is increased. The rigid moiety of cholesterol has a slightly higher electron density than the lipid alkyl chains. This results in a peak due to cholesterol, as found in DPPC–cholesterol mixtures, at around ± 10 Å from the center of the bilayers. However, the increase in the electron density due to the localization of cholesterol in the bilayers is more prominent in the case of DPPC–cholesterol bilayers, as indicated by the secondary maxima at $\sim \pm 10$ Å from the bilayer center, than in DOPC–cholesterol bilayers. This difference between DOPC–cholesterol and DPPC–cholesterol mixtures could be the consequence of the longer and unsaturated chains of DOPC molecules. The presence of a kink in the chains of DOPC might cause inefficient packing of cholesterol and further the short length of cholesterol, compared to DOPC, results in the partial stretching of the chains. Hence the electron density of the broad shallow region due to the terminal methyl group does not elevate significantly, as in the case of DPPC–cholesterol bilayer discussed in chapter 3. Fig. 5.4 shows the electron density profile at $X_c = 30$ mol% as a function of temperature. These profiles clearly indicate that there is no significant change in the bilayer structure with temperature.

The in-plane ordering of the hydrocarbon chains can be inferred from the wide angle reflection, as discussed in the case of DPPC–cholesterol mixtures. We have never seen the wide angle reflections in the L_α phase at lower X_c (< 20 mol%) in the present experimental

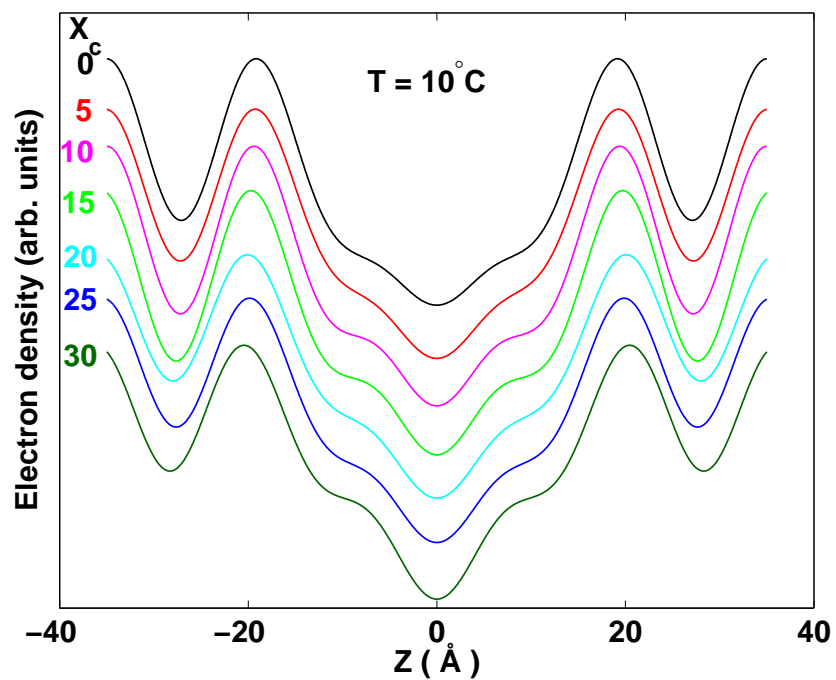


Figure 5.3: Transbilayer electron density profiles obtained from the data given in table 5.2 at different X_c .

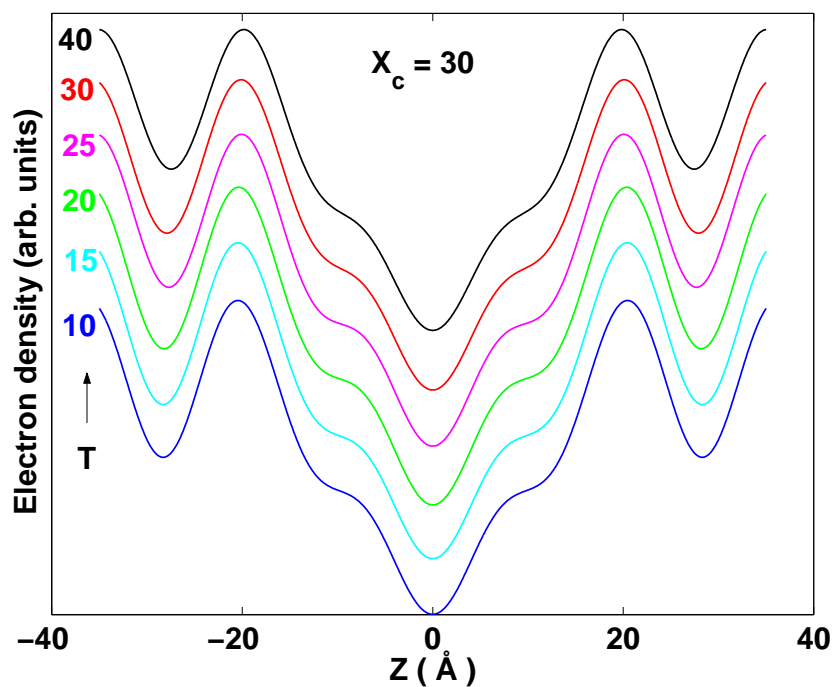


Figure 5.4: Transbilayer electron density profiles obtained from the data given in table 5.3 at $X_c = 30$ mol%, as a function of temperature (RH = 98%).

geometry. However, we have observed diffused wide angle reflections condensed at the equatorial plane for DPPC–cholesterol mixtures at $X_c > 20$ mol%, due to the stretching of the hydrocarbon chains in the L_α phase. We have not seen the wide angle reflections in DOPC–cholesterol mixtures even at higher X_c . As discussed above, the stretching of the hydrocarbon chains in the presence of cholesterol might be less effective in case of DOPC–cholesterol bilayers due to the presence of a kink in the hydrocarbon chains. This is also consistent with the fact that the central trough of the electron density profile due to the terminal methyl groups is broader (Fig. 5.3), compared to DPPC–cholesterol mixtures.

5.5 Conclusion

Oriented multilayers of DOPC–cholesterol mixtures were investigated using x-ray diffraction in order to compare with the l_d phase found in ternary mixtures composed of DPPC, DOPC and cholesterol, to be discussed in chapter 6. Due to the very low T_m (-18.3°C), DOPC and DOPC-cholesterol mixtures exhibit a fluid phase throughout the temperature range studied. Electron density profiles obtained from x-ray diffraction data show a gradual narrowing of the central trough as cholesterol concentration is increased due to the stretching of the chains. Although the calculated phases of the reflections do not change with X_c , relative intensities at a given temperature do change with X_c , indicating changes in membrane properties due to the presence of cholesterol.

Bibliography

- [1] S. L. Veatch and S. L. Keller, *Phys. Rev. Lett.* **89**, 268101 (2002) ; *Biophys. J.* **85**, 3074 (2003).
- [2] S. L. Veatch, I. V. Polozov, K. Gawrisch, and S. L. Keller, *Biophys. J.* **86**, 2910 (2004).
- [3] D. Scherfeld, N. Kahya, and P. Schwille, *Biophys. J.* **85**, 3758 (2003).
- [4] M. Gandhavadi, D. Allende, A. Vidal, S. A. Simon, and T. J. McIntosh, *Biophys. J.* **82**, 1469 (2002).
- [5] P. L. -G. Chong and A. R. Cossins, *Biochim. Biophys. Acta* **772**, 197 (1984).
- [6] L. Thewalt J and M. Bloom, *Biophys. J.* **63**, 1176 (1992).
- [7] J. Gallová, D. Uhríková, A. Islamov, A. Kuklin, and P. Balgavý, *Gen. Physiol. Biophys.* **23**, 113 (2004).
- [8] G. Deinum, H. van. Langen, G. van, Ginkel, and Y. K. Levine, *Biochemistry* **27**, 852 (1988).
- [9] M. Straume and B. J. Litman, *Biochemistry* **26**, 5121 (1987).
- [10] A. Filippov, G. Orädd, and G. Lindblom, *Biophys. J.* **84**, 3079 (2003).
- [11] Y. Liu and J. F. Nagle, *Phys. Rev. E* **69**, 040901 (2004).
- [12] A. Spaar and T. Salditt, *Biophys. J.* **85**, 1576 (2003).
- [13] L. J. Korstanje, G. van Ginkel, and Y. K. Levine, *Biochim. Biophys. Acta* **1022**, 155 (1990).

- [14] R. M. Epanand, D. W. Hughes, B. G. Sayer, N. Borochoy, D. Bach, and E. Wachtel, *Biochim. Biophys. Acta* **1616**, 196 (2003).
- [15] A. Parker, K. H. Miles, K. Cheng, and J. Huang, *Biophys. J.* **86**, 1532 (2004).
- [16] N. Kahya, D. Scherfeld, K. Bacia, B. Poolman, and P. Schwille, *J. Biol. Chem.* **278**, 28109 (2003).
- [17] R. Koynova and M. Caffrey, *Biochim. Biophys. Acta* **1376**, 91 (1998).
- [18] S. Tristram-Nagle, H. I. Petrache, and J. F. Nagle, *Biophys. J.* **75**, 917 (1998).
- [19] T. J. McIntosh, *Biochim. Biophys. Acta* **513**, 43 (1978).